

See discussions, stats, and author profiles for this publication at: <https://www.researchgate.net/publication/229012442>

# 'Simultaneous States and Parameters Estimation of an Ozonation Reactor Based on Dynamic Neural Network

Article in *Differential Equations and Dynamical Systems* · February 2002

CITATIONS

7

READS

47

4 authors, including:



Wen Yu

Center for Research and Advanced Studies of the National Polytechnic Institute

416 PUBLICATIONS 5,449 CITATIONS

SEE PROFILE



Poznyak Tatyana

Instituto Politécnico Nacional

125 PUBLICATIONS 827 CITATIONS

SEE PROFILE

Some of the authors of this publication are also working on these related projects:



Neural PID admittance control of a robot [View project](#)



Fuzzy modelling via on-line support vector machines [View project](#)

# Simultaneous States and Parameters Estimation of an Ozonation Reactor Based on Dynamic Neural Network

A.S. Poznyak, Wen Yu, T.I. Poznyak, and K. Najim

## Abstract

This paper deals with the simultaneous states and parameters estimation of an ozonation reactor using a dynamic neural network and the least squares method. We use a dynamic model derived from mass balance considerations. We propose a continuous time algorithm which includes two parallel procedures: state estimation using a Dynamic Neural Network (DNN) and parameters identification based on Least Squares Method (LSM). A set of numerical simulations has been carried out in order to illustrate the performance of this algorithm.

## 1. Introduction

The design and control of ozonation reactors have always been the challenging tasks mostly because of the inadequacy of on-line sensors with

---

<sup>0</sup>AMS (MOS) 2001 Subject classifications:  
0

fast sampling rate and small time delay (since ozone is the most quick oxidant), and the complex nonlinear strongly interactive behavior of ozonation reactions. The only available measurements concern the concentration of ozone in the gaseous phase of the reactor. To overcome the present limitations of sensors technology (for example, sensors for concentrations measurement are not available or are very expensive since special chromatography devices are required, etc.), a differential neural network is used for state estimation (compound concentrations) [7] [4] [23] [9] [11]. As in many engineering problems, we are concerned with the simultaneous states and parameters estimation for nonlinear systems.

In this paper we propose a continuous time algorithm which includes two parallel procedures: state estimation using a *Differential Neural Network* (DNN) and, parameters identification based on *Least Squares Method* (LSM).

Several studies have been dedicated to the use neural networks techniques for constructing states observers for nonlinear systems. In [3] a nonlinear observer, based on the ideas given in [5], is combined with a feedforward neural network, which is used to solve a matrix equation. In [8] a nonlinear observer is used to estimate the nonlinearities of an input signal. As far as we know, the first observer for nonlinear systems using dynamic neural networks was presented in [10]. The stability of this observer with on-line adaptation of neural network weights is analyzed, but several restrictive assumptions are made: the nonlinear plant must contain a known linear part and a strictly positive real (*SPR*) condition must be fulfilled. In [17] a robust neuro-observer with time delay term and adjusted weights in the hidden layer is presented.

In this paper a Differential Neuro-Observer (DNO) is used for the estimation of the compound concentrations (states). Based on the DNO outputs, the chemical reaction rates are identified using the continuous version of the Least Squares Method (LSM) with a projection procedure. The theoretical analysis of this DNO is carried out using Lyapunov-like technique.

Several simulation results have been carried out in order to illustrate

the feasibility and the efficiency of the presented approach.

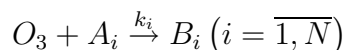
The *remainder* of this paper is organized as follows. The model of the considered ozonation reactor as well as the problem formulation are presented in the next section. Section 3 deals with observability condition for the partial (but more practice) case of  $N = 3$  compounds mixture. The neuro-observer with the corresponding learning law for the weight matrix is described in Section 4. The estimation of the reaction rate constants is discussed in Section 5. Numerical simulations are given in section 6. Section 7 concludes this paper.

## 2. Process Modelling and Problem Formulation

### 2.1. Reactor Model and Measurable Variables

*Ozone-liquid systems* are extensively used in different industrial environmental processes such as wastewater, river and drinking water treatment, etc. The main aim of the ozonation treatment (“purification”) is the quick and effective elimination of hydrocarbon contaminants (paraffins, olefins and aromatic compounds) from the given liquid mixture (for example, water) [1] [19]). Such processes are usually carried out in ozonation reactors under specific temperature and pressure.

The *ozonation reactor*, considered here, represents a semi-batch reactor where the ozone feed enters the bottom as shown in Fig. 1. Several parallel ozonation reactions take place in the reactor [6]:



where  $O_3$  is ozone,  $A_i$  is one of the organic compounds and  $B_i$  is the corresponding ozonation product.

The monotonic decreasing elimination curves for different organic compounds ( $c_t^i$  is the current concentration of the compound  $A_i$ ) are shown in Fig. 2.

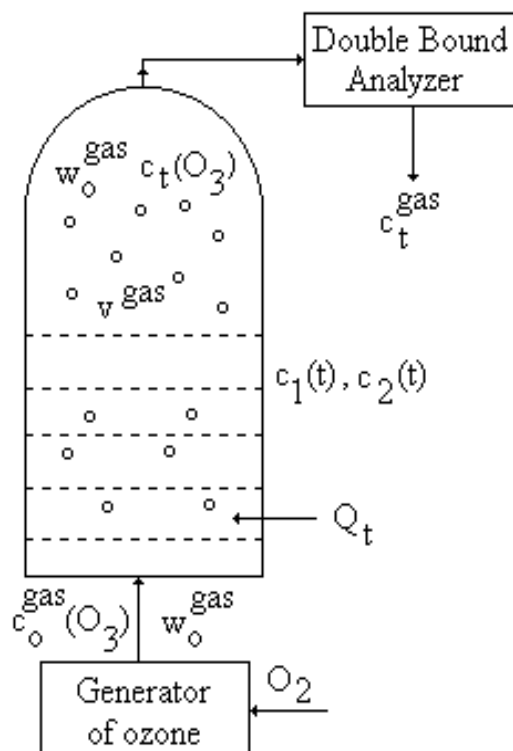


Figure 1: Schematic diagram of the ozonization reactor.

The ozonation process can be stopped at time  $\tau$  if the "contaminant level" for all contaminants does not exceed a given value, namely  $d$ , that is,

$$\tau := \max_{i=1, N} \{t_i : c_{t_i}^i = d\} \quad (1)$$

The *mathematical model* of these processes, developed in [18], is actively applied to ozonation reactor design [20], the efficiency optimization and the prediction of their actual performance [21], operation and maintenance, ensuring safety, and development of control strategies [2] [13].

The model of the considered semi-batch ozonation reactor is described

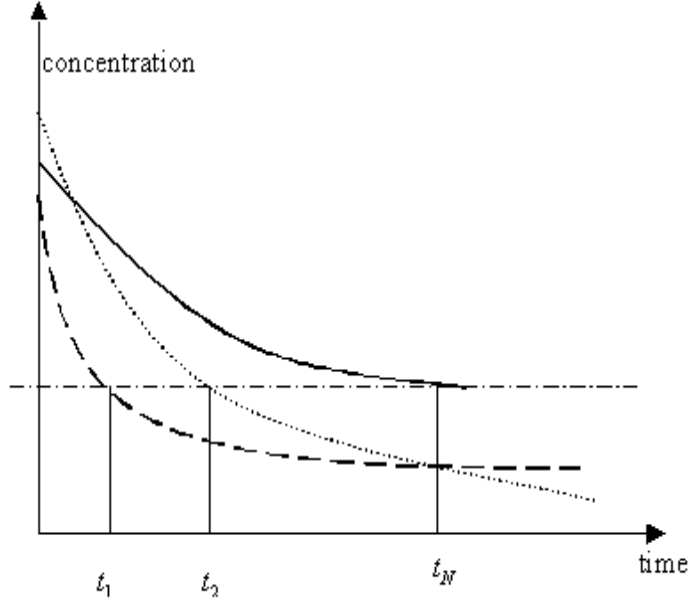


Figure 2: Concentration of different organic compounds.

in what follows.

### 2.1.1. Ozone Mass Balance

The mass balance consideration (with respect to ozone) leads to the following model [18] given in the integral form:

$$\int_{\tau=0}^t w^{gas} c_t^{in} d\tau = \int_{\tau=0}^t w^{gas} c_t^{out} d\tau + c_t^{out} v^{gas} + Q_t + v^{liq} \sum_{i=1}^N (c_0^i - c_t^i) \quad (2)$$

$$c_t^{in} := c_0^{gas} = const, \quad c_t^{out} := c_t^{gas}$$

or, in the equivalent differential form,

$$\frac{d}{dt} c_t^{out} := \frac{1}{v^{gas}} \left\{ w^{gas} [c_t^{in} - c_t^{out}] - \frac{d}{dt} \left[ Q_t + v^{liq} \sum_{i=1}^N (c_0^i - c_t^i) \right] \right\} \quad (3)$$

where  $c_t^i$  (*mole/l*) is the  $i^{th}$  organic compound concentration at time  $t \geq 0$ ,  $i = 1, \dots, N$ ,  $N$  is the number of different organic compounds dissolved in the liquid phase of the given ozonation reactor,  $c_t^{out} := c_t^{gas}$  (*mole/l*) is the gas (moles) which do not react with organic compounds dissolved in the solvent and can be *directly measured* in the outlet of the ozonation reactor,  $w^{gas}$  (*l/s*) is the gas consumption assumed to be constant,  $v^{gas}$  (*l*) is the volume of the gas phase which is assumed to be constant,  $Q_t$  (*mole*) is the dissolved ozone, and  $v^{liq}$  (*l*) is the volume of the liquid phase. It is assumed to be constant.

### 2.1.2. Ozone Dissolution Process

The differential equation associated with the ozone dissolution process is given by:

$$\frac{d}{dt} \left[ Q_t + v^{liq} \sum_{i=1}^N (c_0^i - c_t^i) \right] = K_{sat} [Q_{\max} - Q_t] \quad (4)$$

where  $K_{sat}$  ( $s^{-1}$ ) is the ozone volumetric mass transfer coefficient, and  $Q_{\max} = \alpha c_t^{out} v^{liq}$  (*mole*) is the maximum of ozone being in the saturated ( $t \rightarrow \infty$ ) liquid phase under the given conditions. The parameter  $\alpha$  deduced from the Henry constant.

## 2.2. Organic Compounds Reactions with Ozone

The differential equations describing the bimolecular chemical reactions for each organic compound are [21]:

$$\frac{d}{dt} c_t^i = -k_i c_t^i Q_t / v^{liq} \quad (i = 1, \dots, N) \quad (5)$$

where  $k_i$  ( $ls^{-1}mol^{-1}$ ) is the rate constant of the ozonation reaction related to the  $i^{th}$  organic compound.

## 2.3. Problem Setting

Before the problem formulation, let us introduce two "auxiliar" processes  $\hat{Q}_t$  and  $y_t$ , which may be constructed based on the measurable process  $c_t^{gas}$ .

Substitution of (4) into (3) leads to

$$Q_t = Q_{\max} + K_{sat}^{-1} v^{gas} \frac{d}{dt} c_t^{out} - K_{sat}^{-1} w^{gas} [c_t^{in} - c_t^{out}]$$

Based on Euler approximation, we derive

$$\frac{d}{dt} c_t^{out} \simeq h^{-1} (c_t^{out} - c_{t-h}^{out}), h > 0 \quad (6)$$

$Q_t$  can be estimated as follows

$$\begin{aligned} Q_t &= \hat{Q}_t + v^{liq} \xi_t \\ \hat{Q}_t &:= Q_{\max} + K_{sat}^{-1} v^{gas} h^{-1} (c_t^{out} - c_{t-h}^{out}) - K_{sat}^{-1} w^{gas} (c_t^{in} - c_t^{out}) \end{aligned} \quad (7)$$

where  $\xi_t$  is the unmeasured dynamics related to the approximation (6).  $\xi_t$  is given by

$$\xi_t := (Q_t - \hat{Q}_t) / v^{liq} = K_{sat}^{-1} v^{gas} \left[ \frac{d}{dt} c_t^{out} - h^{-1} (c_t^{out} - c_{t-h}^{out}) \right] / v^{liq} \quad (8)$$

The integration of (4) directly leads to the following expression:

$$S_t := \sum_{i=1}^N c_t^i = \sum_{i=1}^N c_0^i + \frac{1}{v^{liq}} (Q_t - Q_0) - \frac{1}{v^{liq}} \int_{s=0}^t K_{sat} [Q_{\max} - Q_s] ds \quad (9)$$

In view of (7), (9) can be written as follows

$$S_t = y_t + \xi_t \quad (10)$$

where  $y_t$  is given by

$$\begin{aligned} y_t &:= \sum_{i=1}^N c_0^i + (\hat{Q}_t - Q_0) / v^{liq} - [c_t^{in} - c_t^{out}] v^{gas} / v^{liq} \\ &\quad - w^{gas} / v^{liq} \int_{s=0}^t [c_s^{in} - c_s^{out}] ds \end{aligned} \quad (11)$$

So, the processes  $y_t$  and  $\hat{Q}_t$ , related to the considered ozonation reactor and constructed based only on the available measurements of  $c_t^{out}$ , satisfy



$$\begin{cases} Q_t = \hat{Q}_t + v^{liq}\xi_t \\ \xi_t = y_t - S_t \end{cases} \quad (12)$$

The problem which we are dealing with can be formulated as follows: based on the available data  $\{c_t^{out}\}$  (and, hence, on  $\hat{Q}_t$  and  $y_t$ ) construct the estimates  $\hat{c}_t^i$  of the state vector  $c_t^i$  as well as the estimates  $\hat{k}_{i,t}$  of unknown parameters  $k_i$  ( $i = 1, \dots, N$ ) and derive their accuracy bounds.

As already mentioned, reliable sensors for concentrations measurement are not available or are very expensive, an efficient estimation procedure (based only on  $\{c_t^{out}\}$ ) can contribute significantly to the improvement of the reactor monitoring and control. The model of this process is given by

$$\begin{cases} \frac{d}{dt}c_t^i = -k_i c_t^i \left( \hat{Q}_t / v^{liq} + \xi_t \right) & (i = 1, \dots, N) \\ y_t = \sum_{i=1}^N c_t^i - \xi_t \end{cases} \quad (13)$$

and represents the basis for on-line estimation of the current compound concentrations  $c_t^i$  and the identification of the rate constants  $k_i$ .

### 3. Observability Condition

First, to understand whether or not the output signal  $y_t$  contains enough information to estimate the components  $c_t^i$  ( $i = 1, \dots, N$ ), try to obtain, so-called, “*observability condition*”. To do that, consider now the same problem, assuming that  $c_t^{out}$  as well as  $\frac{d}{dt}c_t^{out}$  are available, that is, put  $\xi_t = 0$ . It implies that  $Q_t$  is available too and the considered process model can be rewritten as follows:

$$\begin{cases} \frac{d}{dt}c_t^i = f_t^i(c_t^i) := -k_i c_t^i Q_t / v^{liq} & (i = 1, \dots, N) \\ y_t = \sum_{i=1}^N c_t^i \end{cases} \quad (14)$$

where  $c_t^i$  and  $y_t$  are the states and output of the corresponding dynamic system whose model is given by (14).

Consider the case  $N = 3$  which covers a lot of practical situations. The calculation of the *Lie* derivatives of the time-functions  $\dot{y}_t$  and  $\ddot{y}_t$  along the trajectories of this system leads to

$$\begin{bmatrix} y_t \\ \dot{y}_t \\ \ddot{y}_t \end{bmatrix} = \mathcal{O}_t \begin{bmatrix} c_t^1 \\ c_t^2 \\ c_t^3 \end{bmatrix}$$

where  $\mathcal{O}_t$  is the observability matrix given by

$$\mathcal{O}_t = \begin{bmatrix} 1 & 1 & 1 \\ -\tilde{k}_1 Q_t & -\tilde{k}_2 Q_t & -\tilde{k}_3 Q_t \\ \tilde{k}_1 (\tilde{k}_1 Q_t^2 - \dot{Q}_t) & \tilde{k}_2 (\tilde{k}_2 Q_t^2 - \dot{Q}_t) & \tilde{k}_3 (\tilde{k}_3 Q_t^2 - \dot{Q}_t) \end{bmatrix} \quad (15)$$

$\tilde{k}_i := k_i / v^{liq} \quad (i = 1, \dots, N = 3)$

The states  $c_t^i$  of the system (14) are globally observable if and only if

$$\begin{aligned} \det \mathcal{O}_t &= Q_t \left[ \tilde{k}_1 (\tilde{k}_1 Q_t^2 - \dot{Q}_t) (\tilde{k}_2 - \tilde{k}_3) + \tilde{k}_2 (\tilde{k}_2 Q_t^2 - \dot{Q}_t) (\tilde{k}_3 - \tilde{k}_1) \right. \\ &\quad \left. + \tilde{k}_3 (\tilde{k}_3 Q_t^2 - \dot{Q}_t) (\tilde{k}_1 - \tilde{k}_2) \right] \\ &= Q_t^3 \left[ \tilde{k}_1^2 (\tilde{k}_2 - \tilde{k}_3) + \tilde{k}_2^2 (\tilde{k}_3 - \tilde{k}_1) + \tilde{k}_3^2 (\tilde{k}_1 - \tilde{k}_2) \right] \neq 0 \end{aligned}$$

That is, the process  $y_t$  contains the sufficient information to estimate the states  $c_t^i$  if  $Q_t$  is not equal to zero and all reaction rates are different:

$$(Q_t \neq 0) \wedge (k_2 \neq k_3) \wedge (k_1 \neq k_2) \wedge (k_1 \neq k_3) \quad (16)$$

## 4. Neuro-Observer

### 4.1. Neuro-Observer Structure

According to [22] [14] [15], consider the dynamic neuro-observer given by

$$\begin{cases} \frac{d}{dt} \hat{x}_t = A \hat{x}_t + W_t \sigma(\hat{x}_t) + K [y_t - \hat{y}_t] \\ \hat{y}_t = C^T \hat{x}_t, \quad C^T = (1, \dots, 1) \in \mathcal{R}^n \end{cases} \quad (17)$$

where  $\hat{x}_t \in \mathcal{R}^n$  is the state of the observer interpreted as the current estimate of the state vector  $c_t = (c_t^1, \dots, c_t^N)^\top$ ,  $A \in \mathcal{R}^{n \times n}$  is a matrix to be selected,  $\sigma : \mathcal{R}^n \rightarrow \mathcal{R}^k$  a smooth vector field usually represented by the sigmoid of the form

$$\sigma_i(x) = \frac{a_i}{1 + e^{-b_i^\top x}} - c_i \quad (18)$$

$W_t \in \mathcal{R}^{n \times k}$  is the weight matrix to be adjusted by a learning procedure,  $y_t$  is given by (11) and  $K$  is the observer gain matrix to be selected. The parameters  $a_i$ ,  $b_i$  and  $c_i$  are assumed to be *a priori* given or selected during the experiment by "try-to-test" method. The sigmoid vector functions  $\sigma(\cdot)$ , commonly used in neural networks as the activation function, satisfy the Lipschitz condition ( $\forall x', x'' \in \mathcal{R}^n$ )

$$\begin{aligned} \tilde{\sigma} &:= \sigma(x') - \sigma(x'') \\ \tilde{\sigma}^\top \Lambda_\sigma \tilde{\sigma} &\leq (x' - x'')^\top D_\sigma (x' - x'') \end{aligned}$$

where  $\Lambda_\sigma = \Lambda_\sigma^\top > 0$ ,  $D_\sigma = D_\sigma^\top > 0$  are known normalizing matrices. The structure of the neuro-observer is shown in Fig. 3.

## 4.2. Basic Assumptions

**A1:** The pair  $(A, C)$  is detectable, that is, there exists a matrix  $K$  such that the combined matrix  $\mathcal{A} := A - KC^\top$  is stable (Hurwitz).

**A2:** There exist a gain matrix  $K$ , strictly positive defined matrices  $\bar{Q}$ ,  $\Lambda_1$ ,  $\Lambda_\varphi$  and a positive  $\delta > 0$  such that the matrix Riccati equation

$$Ric := P\mathcal{A} + \mathcal{A}^\top P + P\mathcal{R}P + \mathcal{Q} = 0 \quad (19)$$

with

$$\mathcal{A} := A - KC^\top \text{ - a stable matrix}$$

$$\mathcal{R} := \Lambda_1^{-1} + \Lambda_\varphi^{-1} + W^* \Lambda_\sigma^{-1} W^{*\top}$$

$$W^* = W_0 \text{ - an initial weight matrix}$$

$$\mathcal{Q} := D_\sigma + \bar{Q} + \delta I$$

has a positive definite solution  $P$ .

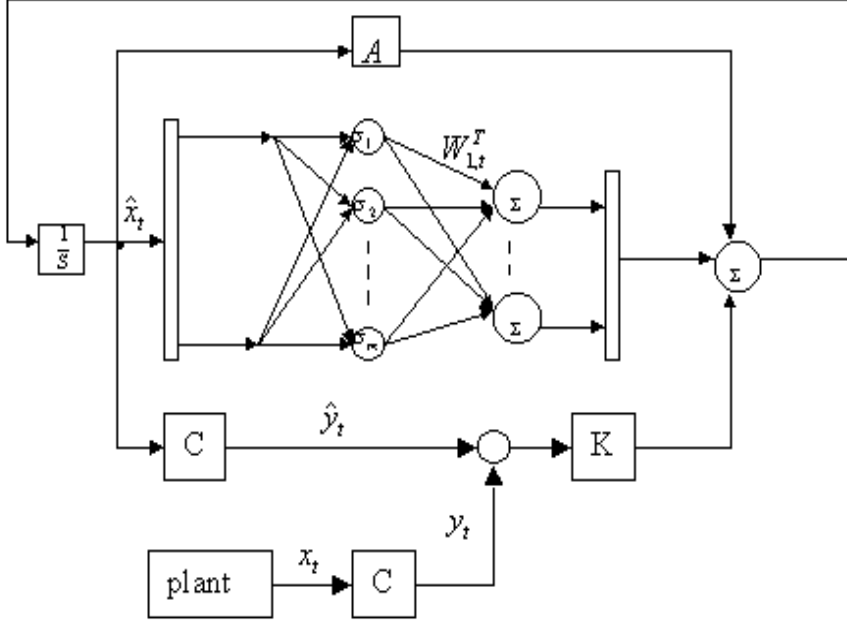


Figure 3: Neuro-observer structure.

### 4.3. Learning Law

Let the weight matrix  $W_t$  be adjusted as follows:

$$\begin{aligned} \dot{W}_t = & DP (N_\delta^{-1})^\top (2 (C^+)^T e_t \\ & - [(C^+)^T \Lambda_\xi^{-1} C^+ + \delta I]^\top N_\delta^{-1} P (W_t - W^*) \sigma(\hat{x}_t)) \sigma^\top(\hat{x}_t) \end{aligned} \quad (20)$$

where  $e_t$  is the output observation error given by

$$e_t := y_t - C^T \hat{x}_t$$

$$N_\delta := CC^+ + \delta I, \quad \delta > 0, \quad C^+ = C^\top / \|C\|^2 = C^\top / N$$

and  $\Lambda_\xi$  any positive definite matrix satisfying  $\xi_t^\top \Lambda_\xi \xi_t \leq 1$  ( $\xi_t$  is defined by (12)). In practice,  $\Lambda_\xi$  can selected as  $\Lambda_\xi = \lambda I$  where  $\lambda$  is a small enough positive scalar.

#### 4.4. Upper Bound for Estimation Error

**Theorem 4.1.** If, under assumptions **A1-A2**, the updating law is given by (20), then the averaged observation error satisfies the following performance:

$$\begin{aligned} \overline{\lim}_{T \rightarrow \infty} \frac{1}{T} \int_0^T \Delta_t^T \bar{Q} \Delta_t dt &\leq \bar{\eta} := \overline{\lim}_{T \rightarrow \infty} \frac{1}{T} \int_0^T \eta_t dt \\ \eta_t &:= \xi_t^T (K^T \Lambda_1^{-1} K + \Lambda_\xi) \xi_t + \varphi_t^T \Lambda_\varphi \varphi_t \\ \varphi_t &:= [W^* \sigma(c_t) + A c_t - f_t(c_t)] \end{aligned} \quad (21)$$

**Proof.** From (12) and (17), it follows

$$\begin{aligned} \dot{\Delta}_t &= A \hat{x}_t + W_t \sigma(\hat{x}_t) + K [y_t - C^T \hat{x}_t] - f_t(c_t) \\ &= (A - K C^T) \Delta_t - K \xi_t + \tilde{W}_t \sigma(\hat{x}_t) \\ &\quad + W^* [\sigma(\hat{x}_t) - \sigma(c_t)] + [W^* \sigma(c_t) + A c_t - f_t(c_t)] \end{aligned} \quad (22)$$

where  $\tilde{W}_t := W_t - W^*$ . Consider the Lyapunov function given by

$$V_t := V(\Delta_t, \tilde{W}_t) := \Delta_t^T P \Delta_t + \frac{1}{2} \text{tr} \left\{ \tilde{W}_t^T D^{-1} \tilde{W}_t \right\}, \quad D = D^T > 0 \quad (23)$$

which derivative, calculated over the trajectories of (22), satisfies

$$\dot{V}_t = \dot{V}(\Delta_t, \tilde{W}_t) = 2 \Delta_t^T P \dot{\Delta}_t + \text{tr} \left\{ \left( \frac{d}{dt} \tilde{W}_t^T \right) D^{-1} \tilde{W}_t \right\} \quad (24)$$

The substitution of (22) into (24) implies:

1)

$$2 \Delta_t^T P (A - K C^T) \Delta_t = \Delta_t^T [P (A - K C^T) + (A - K C^T)^T P] \Delta_t \quad (25)$$

2)

$$-2 \Delta_t^T P K \xi_t \leq \Delta_t^T P \Lambda_1^{-1} P \Delta_t + \xi_t^T K^T \Lambda_1^{-1} K \xi_t \quad (26)$$

(here the inequality

$$X^T Y + Y^T X \leq X^T \Lambda^{-1} X + Y^T \Lambda Y \quad (27)$$

which is valid for any  $X, Y \in \mathcal{R}^{n \times m}$  and any  $\Lambda = \Lambda^\top \in \mathcal{R}^{n \times n}$ , is applied).

3) by (27) it follows

$$\begin{aligned}
2\Delta_t^\top P\tilde{W}_t\sigma(\hat{x}_t) &= 2(-e_t^\top C^+ N_\delta^{-1} - \xi_t^\top C^+ N_\delta^{-1} + \delta\Delta_t^\top N_\delta^{-1}) P\tilde{W}_t\sigma(\hat{x}_t) \\
&= -tr \left\{ 2\sigma(\hat{x}_t) e_t^\top C^+ N_\delta^{-1} P\tilde{W}_t \right\} \\
&\quad - 2\xi_t^\top C^+ N_\delta^{-1} P\tilde{W}_t\sigma(\hat{x}_t) + 2\delta\Delta_t^\top N_\delta^{-1} P\tilde{W}_t\sigma(\hat{x}_t) \\
&\leq -tr \left\{ 2\sigma(\hat{x}_t) e_t^\top C^+ N\delta^{-1} P\tilde{W}_t \right\} \\
&\quad + \sigma^\top(\hat{x}_t) \tilde{W}_t^\top P (N_\delta^{-1})^\top (C^+)^\top \Lambda_\xi^{-1} C^+ N_\delta^{-1} P\tilde{W}_t\sigma(\hat{x}_t) \\
&\quad + \xi_t^\top \Lambda_\xi \xi_t + \delta\Delta_t^\top \Delta_t + \delta\sigma^\top(\hat{x}_t) \tilde{W}_t^\top P (N_\delta^{-1})^\top N_\delta^{-1} P\tilde{W}_t\sigma(\hat{x}_t) \\
&= tr \left\{ \sigma(\hat{x}_t) \left[ -2e_t^\top C^+ + \sigma^\top(\hat{x}_t) \tilde{W}_t^\top P (N_\delta^{-1})^\top \right. \right. \\
&\quad \times \left. \left. \left[ (C^+)^\top \Lambda_\xi^{-1} C^+ + \delta I \right] \right] N_\delta^{-1} P\tilde{W}_t \right\} + \xi_t^\top \Lambda_\xi \xi_t + \delta\Delta_t^\top \Delta_t
\end{aligned}$$

since

$$\begin{aligned}
e_t &:= y_t - C^\top \hat{x}_t = -C^\top \Delta_t - \xi_t \\
\Delta_t^\top C &= -e_t^\top - \xi_t^\top
\end{aligned}$$

and

$$\begin{aligned}
\Delta_t^\top &= \Delta_t^\top N_\delta N_\delta^{-1} = \Delta_t^\top (CC^+ + \delta I) N_\delta^{-1} \\
&= -e_t^\top C^+ N_\delta^{-1} - \xi_t^\top C^+ N_\delta^{-1} + \delta\Delta_t^\top N_\delta^{-1} \\
N_\delta &:= CC^+ + \delta I, \quad \delta > 0
\end{aligned}$$

(  $C^+$  represents the pseudo-inverse of  $C$  ).

4) by the property of the sigmoid function, we derive

$$\begin{aligned}
2\Delta_t^\top PW^* [\sigma(\hat{x}_t) - \sigma(c_t)] &\leq \Delta_t^\top PW^* \Lambda_\sigma^{-1} W^{*\top} P \Delta_t \\
&\quad + [\sigma(\hat{x}_t) - \sigma(c_t)]^\top \Lambda_\sigma [\sigma(\hat{x}_t) - \sigma(c_t)] \\
&\leq \Delta_t^\top (PW^* \Lambda_\sigma^{-1} W^{*\top} P + D_\sigma) \Delta_t
\end{aligned}$$

5) for the term  $\varphi_t := [W^* \sigma(c_t) + Ac_t - f_t(c_t)]$ , tending to zero in view of (5), it follows:

$$2\Delta_t^\top P\varphi_t \leq \Delta_t^\top P\Lambda_\varphi^{-1} P\Delta_t + \varphi_t^\top \Lambda_\varphi \varphi_t$$

Adding and substracting the term  $\Delta_t^\top \bar{Q} \Delta_t$  ( $\bar{Q} = \bar{Q}^\top > 0$ ) from the right-hand side of (24), we obtain:

$$\dot{V}_t \leq \Delta_t^\top Ric \Delta_t + tr \left[ L_t + \frac{d}{dt} \left( \widetilde{W}_t \right)^\top D^{-1} \right] - \Delta_t^\top \bar{Q} \Delta_t + \eta_t$$

where

$$L_t := \sigma(\hat{x}_t) \left[ -2e_t^\top C^+ + \sigma^\top(\hat{x}_t) \tilde{W}_t^\top P (N_\delta^{-1})^\top \left[ (C^+)^\top \Lambda_\xi^{-1} C^+ + \delta I \right] \right] N_\delta^{-1} P$$

$$\eta_t := \xi_t^\top (K^\top \Lambda_1^{-1} K + \Lambda_\xi) \xi_t + \varphi_t^\top \Lambda_\varphi \varphi_t$$

By **A2** and by the updating law (20), it follows that  $Ric = 0$  and  $DL_t^\top = -\frac{d}{dt} \widetilde{W}_t$ , that implies

$$\dot{V}_t \leq -\Delta_t^\top \bar{Q} \Delta_t + \eta_t \quad (28)$$

Integrating (28) over the interval  $[0, T]$ , and dividing both side by  $T$ , we finally obtain

$$T^{-1} (V_T - V_0) \leq -T^{-1} \int_{s=0}^T \Delta_s^\top \bar{Q} \Delta_s ds + T^{-1} \int_{s=0}^T \eta_s ds$$

that leads to the following estimate:

$$T^{-1} \int_{s=0}^T \Delta_s^\top \bar{Q} \Delta_s ds \leq T^{-1} \int_{s=0}^T \eta_s ds - T^{-1} (V_T - V_0)$$

$$\leq T^{-1} \int_{s=0}^T \eta_s ds + T^{-1} V_0$$

Theorem is proven.

A remark is in order at this point.

**Remark 4.2.** The upper bound  $\bar{\eta}$  for the averaged quadratic estimation error can be done less than any  $\varepsilon > 0$  since  $\varphi_t \rightarrow 0$  by (5) and  $\xi_t$  can be done small enough by the selection of the time-interval  $h$  in the approximation (6).

The main concern of the next section is the estimation of the parameters (reaction rate constants).

## 5. Identification of the Reaction Rate Constants

From the previous sections, it follows that the neuro-observer (17) can be used to identify (estimate) the chemical reaction rates (14). Observe that  $\hat{x}_t = \hat{c}_t$  as well as  $d\hat{x}_t/dt$  are given by the neuro-observer. In these conditions, we are ready to define the *LS*-estimates  $\hat{k}_i(t)$  as the following optimization problem:

$$\left(\hat{k}_1(t), \dots, \hat{k}_N(t)\right) := \arg \min_{k_i} \int_{s=0}^t \sum_{i=1}^N \left( \frac{d\hat{x}_s^i}{ds} + k_i \hat{x}_s^i \hat{Q}_s v_{liq}^{-1} \right)^2 ds \quad (29)$$

whose solution satisfies (with  $o(\eta)$ -approximation) the following differential equation:

$$\begin{aligned} \frac{d}{dt} \tilde{K}_t &= \left( \frac{d}{dt} \hat{x}_t - \hat{K}_t \hat{x}_t \hat{Q}_t / v^{liq} \right) \hat{x}_t^T \Gamma_t \hat{Q}_t / v^{liq} \\ \dot{\Gamma}_t &= -\Gamma_t \hat{x}_t \hat{x}_t^T \Gamma_t \left( \hat{Q}_t / v^{liq} \right)^2, \quad \Gamma_0 = \eta^{-1} I \\ \tilde{K}_t &:= \text{diag} \left( \tilde{k}_{1,t}, \dots, \tilde{k}_{N,t} \right) \\ \hat{K}_t &= \begin{bmatrix} \hat{k}_{1,t} = \left[ \tilde{k}_{1,t} \right]_+ & 0 & \cdot & 0 \\ 0 & \cdot & 0 & 0 \\ 0 & 0 & \cdot & 0 \\ 0 & \cdot & 0 & \hat{k}_{N,t} \left[ \tilde{k}_{N,t} \right]_+ \end{bmatrix} \end{aligned} \quad (30)$$

where  $\eta$  is a small enough positive constant and the function  $[\cdot]_+$  is defined as follows

$$[z]_+ := \begin{cases} z & \text{if } z \geq 0 \\ 0 & \text{if } z < 0 \end{cases} \quad (31)$$

From an initial condition  $\hat{K}_0$ , we calculate the diagonal elements of  $\hat{K}_t$  on-line, using  $\hat{Q}_t$  and  $\hat{x}_t$  generated by (7) and (17), respectively.

**Remark 5.1.** This algorithm generates the continuous-time Least Squares estimates with a special projection procedure (31).

The next section presents the simulation results.



## 6. Simulation Results

The simulation experiments described in this section are intended to illustrate the main results presented previously. The estimation algorithms described and analyzed in this paper are easy to code since they have few adjustable (design) parameters: the matrices  $A, \Lambda_1, \Lambda_\varphi, W^*, \Lambda_\sigma, K, D$  and the scalars  $\delta$  and  $\eta$ .

### 6.1. Experiment 1 (Medium Rate Process)

This experiment has been carried out using the following values for the parameters associated with the ozonation reactor (3),(5):

$c_o^1 = 1 \times 10^{-5}$	$c_o^2 = 1 \times 10^{-5}$	$Q_o = 10^{-8}$	$c_o^{in} = 1 \times 10^{-6}$
$k_1 = 10^5$	$k_2 = 10^4$	$K_{sat} = 0.2$	$Q_{\max} = 1.68 \times 10^{-8}$
$v_{liq} = 8 \times 10^{-3}$	$v_{gas} = 6 \times 10^{-3}$	$w_{gas} = 1.94 \times 10^{-3}$	

- First, we check the identification ability of the neural network for this chemical system.

If the system is observable, we may construct a dynamical neural network to estimate  $c_t^1$  and  $c_t^2$ . The neural network is the same as in (17) ( $n = 4$ ). The experiments reported herein have been carried out for the following values

$$A = \text{diag}[-2, -2, -2, -2], \quad \sigma(\hat{x}_i) = 2 / (1 + e^{-2\hat{x}_i}) - 0.5$$

$$K = [3, 3]^T, \quad \hat{x}_0 = [10^{-5}, 10^{-5}]$$

The algorithm was designed with the following parameters  $\bar{\eta} = 2$ ,  $Q_0 = I_4$ ,  $\Lambda_1^{-1} = 2I_4$ ,  $\Lambda_\xi = 0.1I$

$$\bar{W}_1 = \begin{bmatrix} 3 & 0.1 & 0.1 & 0.1 \\ 0.1 & 3 & 0.1 & 0.1 \\ 0.1 & 0.1 & 3 & 0.1 \\ 0.1 & 0.1 & 0.1 & 3 \end{bmatrix} \quad \text{and} \quad D_\sigma = \begin{bmatrix} 1 & 0.1 & 0.1 & 0.1 \\ 0.1 & 1 & 0.1 & 0.1 \\ 0.1 & 0.1 & 1 & 0.1 \\ 0.1 & 0.1 & 0.1 & 1 \end{bmatrix}.$$

These design parameters gave good results. For the Riccati equation (19), we obtain the following solution:

$$P = \begin{bmatrix} 0.3477 & 0.01 & 0.01 & 0.01 \\ 0.01 & 0.3477 & 0.01 & 0.01 \\ 0.01 & 0.01 & 0.3477 & 0.01 \\ 0.01 & 0.01 & 0.01 & 0.3477 \end{bmatrix}.$$

$W_{1,t}$  is updated according to the procedure (20) with  $D = dI$ ,  $d = 5$ .

The initial weights have been selected as follows:

$$W_{1,0} = \begin{bmatrix} 10^{-5} & 10^{-6} & 0 & 0 \\ 10^{-6} & 10^{-5} & 0 & 0 \\ 0 & 0 & 10^{-5} & 10^{-5} \\ 0 & 0 & 10^{-5} & 10^{-5} \end{bmatrix}.$$

The time evolution of the weights are shown in Fig. 4.

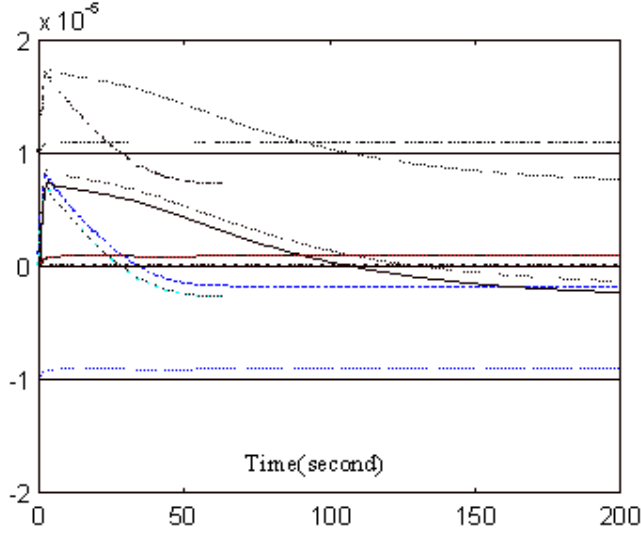
The identification results are shown in Figs. 5-7.

These figures represent the evolution of  $c_t^1$ ,  $c_t^2$ ,  $Q_t$ ,  $c_t^{out}$  and  $W_{1,t}$ . They highlight the performance of the identification procedure. For example, the concentration  $c_t^1$  tends to zero after approximately 65 iterations.

- Second, we check the neuro-observer ability to estimate the states of the ozonation reactor.

If  $c_t^{out}$  is only measurable, we use the model (14). Because  $k_1$  and  $k_2$  are also unknown, we need to construct first a neuro-observer to estimate  $c_t^1$  and  $c_t^2$ . The neural observer is the same as in (17) ( $n = 2$ ). The design parameters have been selected as follows:

$$A = \text{diag}[-2, -2], C = [1, 1], N = \frac{1}{2} \begin{bmatrix} 1 & 1 \\ 1 & 1 \end{bmatrix},$$

Figure 4: Evolution of  $W_{1,t}$ .

$$\sigma(\hat{x}_i) = 2 / (1 + e^{-2\hat{x}_i}) - \frac{1}{2}, \hat{x}_0 = [10^{-5}, 10^{-5}]^T, K = [3, 3]^T,$$

$$\overline{W}_1 = \begin{bmatrix} 3 & 0.1 \\ 0.1 & 3 \end{bmatrix}, \Lambda_1^{-1} = 2I_2, Q_0 = I_2, D_\sigma = \begin{bmatrix} 1 & 0.1 \\ 0.1 & 1 \end{bmatrix}, \delta = 0.1.$$

Observe that  $\mathcal{A} = A - KC$  is stable. The solution of the Riccati equation (19) is

$$P = \begin{bmatrix} 0.3614 & 0.01 \\ 0.01 & 0.3614 \end{bmatrix}.$$

$W_{1,t}$  is updated as in (20) with

$$\widetilde{W}_{1,0} = 0, W_{1,0} = \begin{bmatrix} 7.25 \times 10^{-6} & -1.09 \times 10^{-6} \\ -1.75 \times 10^{-6} & 7.91 \times 10^{-6} \end{bmatrix}$$

The observer results are shown in Fig. 8. The continuous lines represent the estimations. The estimations  $\hat{c}_t^1$  and  $\hat{c}_t^2$  of the states  $c_t^1$  and  $c_t^2$

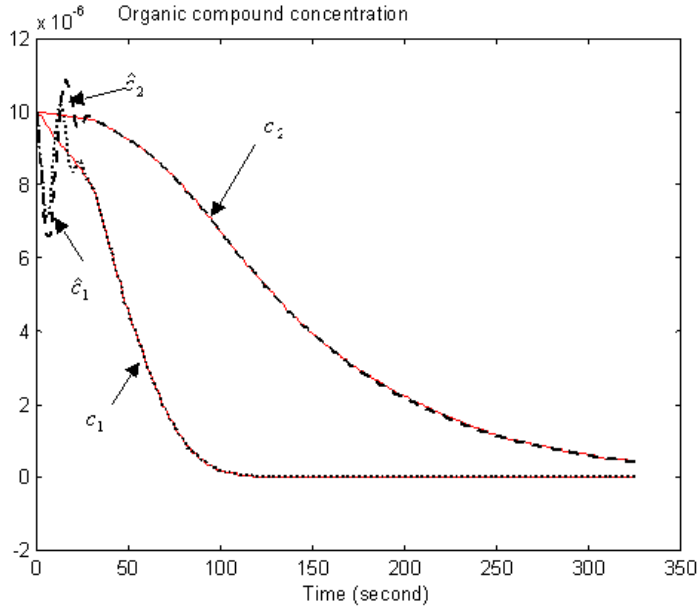


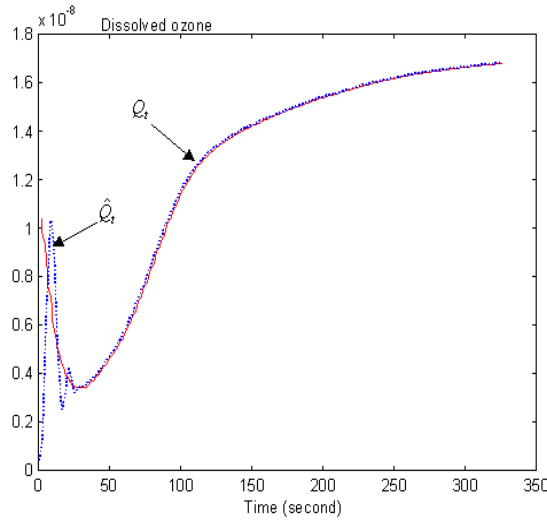
Figure 5: Identification: evolution of  $c_t^1$  and  $c_t^2$ .

given by the neuro-observer are in close agreement with the simulation data carried out from the dynamic model of the ozonation reactor.

These simulation results show the efficiency of the approach presented in this paper. The neuro-observer is able to give good estimates of the non measurable states of the considered chemical reactor. Owing to its ability to give a good estimates of the states, the neuro-observer can be used for other applications.

- Third, we check the least squares estimation ability to estimate the reaction rate constants for this chemical system. Based on (30), we use the estimations  $\hat{c}_t^1$ ,  $\hat{c}_t^2$  and  $\hat{Q}_t$  to identify (estimate) the reaction rate constants  $k_1$  and  $k_2$ . The design parameters are selected as follows:

$$\eta = 10^{16}, \hat{K}_0 = \begin{bmatrix} 0.1 & 0 \\ 0 & 0.1 \end{bmatrix}.$$

Figure 6: Identification: evolution of  $Q_t$ .

The estimation results are depicted in Fig. 9. The estimated constants  $k_1$  and  $k_2$  converge after approximately 1000 iterations. Notice that these constants are the key feature of the dynamic behaviour of the reactor. This figure shows that it is easy to estimate the constants  $k_1$  and  $k_2$  without computational burden.

## 6.2. Experiment 2 (High Rate Process)

Now consider the same reactor with

$$k_1 = 10^6, \quad k_2 = 10^5$$

(the other parameters remain unchanged). As before, we use the same neuro-observer and the  $LS$ -method. The simulation results are shown in Figs. 7-10. These figures indicate, respectively, how  $c_t^1$ ,  $c_t^2$ ,  $W_{1,t}$ ,  $\hat{k}_1$ , and  $\hat{k}_2$  evolve with stage (iteration) number.

The constants  $k_1$  and  $k_2$  are well estimated.

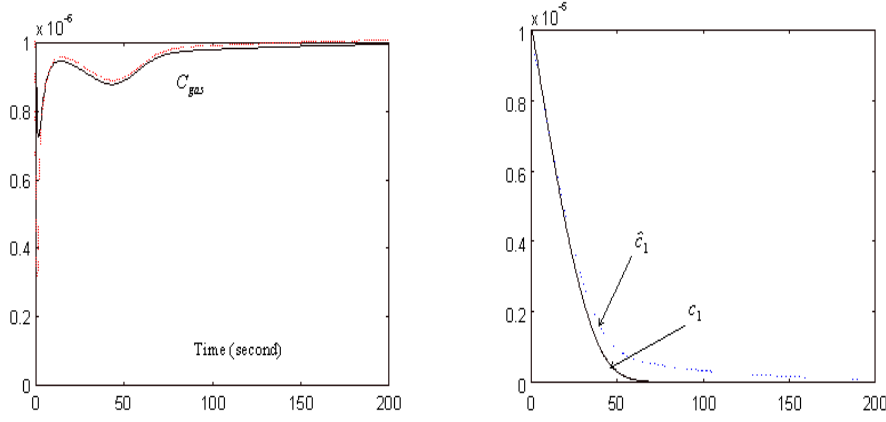


Figure 7: Identification: evolution of  $c_t^{out}$ . Neuro observer for the concentration  $c_t^1$ .

Since the considered system (ozonation reactor) is asymptotically stable, the presented observer is meaningful only when the convergence of the state estimation error to the guaranteed tolerance zone is faster than the dynamics of the process. The numerical experiments show that the dynamics of the neuro-observer are faster than those associated with the ozonation reactor.

## 7. Conclusions

A DNN-observer and a continuous least squares algorithm with a projection procedure have been presented for the simultaneous states and parameters estimation of an ozonation reactor. The analysis of the estimation error for this neuro-observer has been carried out. Several simulation results illustrate the performance and the feasibility of this estimation algorithm. The algorithm presented in this paper is used

- when the concentration sensors are not available or are very expensive;
- for the implementation of state-feedback controllers;

- etc.

The estimation algorithm, described and analyzed in this paper, can find potential applications in many industries such as chemical, mineral, etc.

## References

- [1] P. S. Bailey, Reactivity of ozone with various organic functional groups important to water purification, Proceedings of the 1-st Int. Symposium on Ozone for Water and Wastewater Treatment, Stamford, CT: Int. Ozone Assoc., Pan American Group, pp. 101-117, 1975.
- [2] D. Bonvin, R. G. Rinker and D. A. Mellichamp, On controlling an autothermal fixed-bed reactor at an unstable state - 1, Chemical Engineering Science, 38 (1983), 233-244.
- [3] J. de Leon, E. N. Sanchez, and A. Chataigner, Mechanical system tracking using neural networks and state estimation simultaneously. Proc. 33<sup>rd</sup> IEEE CDC, pp. 405-410, 1994.
- [4] S. Elanayar V.T. and Y. C. Shin, Approximation and estimation of nonlinear stochastic dynamic systems using radial basis function neural network, IEEE Trans. on Neural Networks, 5 (1994), 594-603.
- [5] J. P. Gauthier, H. Hammouri, and S. Othman, A simple observer for nonlinear systems: applications to bioreactors, IEEE Trans. on Automatic Control, 37 (1992), 875-880.
- [6] J. Hoigné and H. Barder, Rate constants of reactions of ozone with organic and inorganic compounds in water -I., Water Res., 17 (1981), 185 - 192.
- [7] K. J. Hunt, D. Sbarbaro, R. Zbinkowski, and P. J. Gawthrop, Neural networks for control systems - A survey, Automatica, 28 (1992), 1083-1112.

- [8] W. L. Keerthipala, H. C. Miao, and B. R. Duggal, An efficient observer model for field oriented induction motor control, Proc. IEEE Trans. SMC, pp. 165-170, 1995.
- [9] G. Lera, A state-space-based recurrent neural network for dynamic system identification, J. of Systems Engineering, 6 (1996), 186-193.
- [10] F. L. Lewis, A. Yesildirek, and K. Liu, Neural net robot controller with guaranteed tracking performance, IEEE Trans. Neural Networks, 6 (1995), 703-715.
- [11] A. U. Levin and K. S. Narendra, Control of nonlinear dynamical systems using neural networks - Part II: Observability, identification, and control, IEEE Trans. on Neural Networks, 7 (1996), 30-42.
- [12] K. Najim, "Control of Liquid-liquid Extraction Columns", Gordon and Breach, London, 1988.
- [13] K. Najim, "Process Modeling and Control in Chemical Engineering", Marcel Dekker, New York, 1989.
- [14] A. S. Poznyak, Learning for dynamic neural networks, 10<sup>th</sup> Yale Workshop on Adaptive and Learning System, pp. 38-47, 1998.
- [15] A. S. Poznyak, W. Yu, E. N. Sanchez, and J. P. Perez, Stability analysis of dynamic neural control, Expert System with Applications, 14 (1998), 227-236.
- [16] A. S. Poznyak, Wen Yu, Edgar N. Sanchez, and Jose P. Perez, Identification via dynamic neural control, IEEE Transactions on Neural Networks, 10 (1999), 1402-1411.
- [17] A. S. Poznyak and Wen Yu, Robust asymptotic neuro observer with time delay term, Int.J. of Robust and Nonlinear Control, 10 (2000), 535-559.
- [18] T. I. Poznyak, D. M. Lisitsyn, and F. S. D'yachkovskii, Selective detector for unsaturated compounds for gas chromatography, J. Anal. Chem., 34 (1979), 2028-2034.



- [19] T. I. Poznyak and J. L. Vivero Escoto, Simulation and Optimization of Phenol and Chlorophenols Elimination from Wastewater. Proceedings of the IOA/PAG Conference, Vancouver, Canada, (18-21 October), 1998, pp. 615 - 628.
- [20] T. I. Poznyak and J. L. Vivero Escoto, Modeling and Optimization of Ozone Mass Transfer in Semibatch Reactor, Proceedings of the International Specialized Symposium of IOA/ EA3G "Fundamental and Engineering Concepts for Ozone Reactor Design" (March 1-3, Toulouse), France, 2000, pp. 133-136.
- [21] T. I. Poznyak and A. Manzo Robledo, Kinetic Study of the Unsaturated Hydrocarbon Pollutants Elimination by Ozonation Method: Simulation and Optimization. Proceedings of the IOA/ PAG Conference, Vancouver, Canada, (18-21 October), 1998, pp. 301 - 311.
- [22] A. Rovithakis and M. A. Christodoulou, Adaptive control of unknown plants using dynamical neural networks, IEEE Trans. on Syst., Man and Cybern., 24 (1994), 400-412.
- [23] J. Sjöberg, Q. Zhang, L. Ljung, A. Benveniste and B. Delyon, Non-linear black-box modelling in system identification: a unified overview, Automatica, 31 (1995), 1691-1724.

**A. S. Poznyak and Wen Yu:** CINVESTAV-IPN, Departamento de Control Automatico, A.P. 14-740, CP 07000 México D.F., México,  
**E-mail:** apoznyak(yuw)@ctrl.cinvestav.mx

**T. I. Poznyak:** E.S.I.Q.I.E.-IPN, Edif. 7 Unidad Profesional Adolfo Lopez M., C.P. 07738 México D.F., México,  
**E-mail:** tpoznyak@hotmail.com

**K. Najim:** Process Control Laboratory, E.N.S.I.A.C.E.T., 118, route de Narbonne, 31077 Toulouse cedex 4, France,  
**E-mail:** Kaddour.Najim@ensiacet.fr.

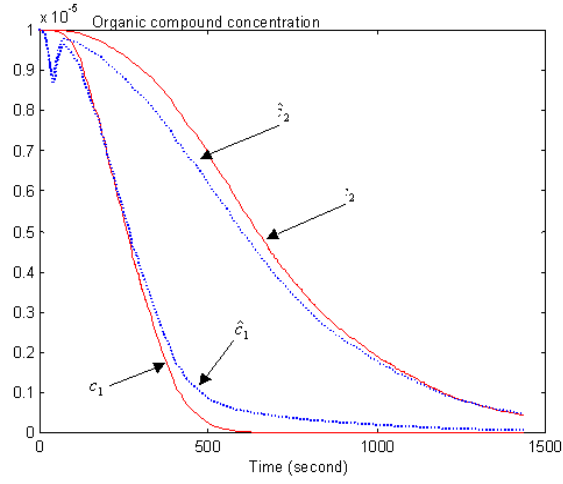


Figure 8: Neuro observer for the concentrations  $c_t^1$  and  $c_t^2$ .

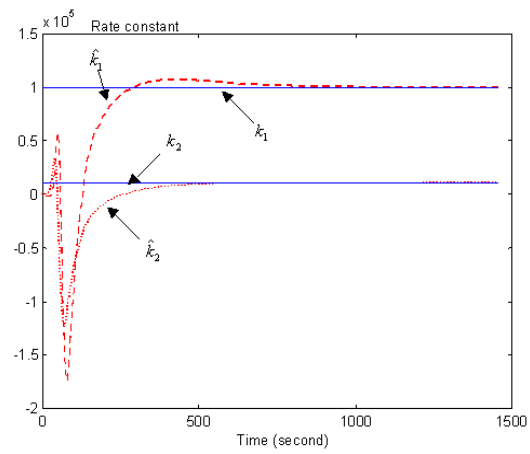


Figure 9: Estimations of  $k_1$  and  $k_2$ .

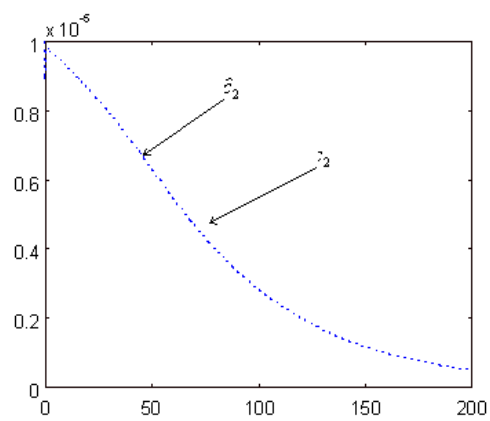
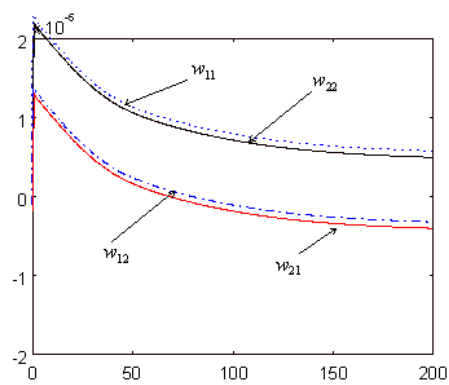
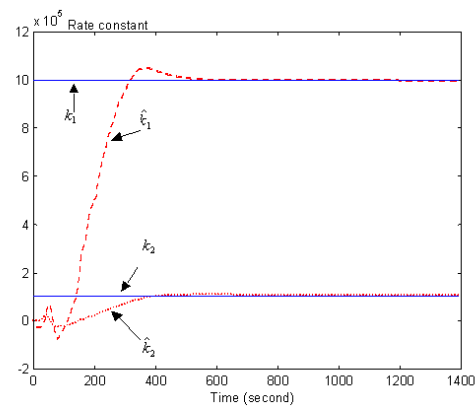


Figure 10: Identification: evolution of  $c_t^{out}$ .



The evolution of  $W_{1,t}$ .



The Estimations of  $k_1$  and  $k_2$ .